Research Square

Preprints are preliminary reports that have not undergone peer review.
They should not be considered conclusive, used to inform clinical practice,
or referenced by the media as validated information.

Octave-Band Characterisation of Heterogeneous Traffic Noise at Urban Intersections

Bhanu Chaudhary

bhanuchaudhary40@gmail.com

Sardar Vallabhbhai National Institute of Technology

Bhaven N. Tandel

Sardar Vallabhbhai National Institute of Technology

Manoranjan Parida

Indian Institute of Technology Roorkee

Research Article

Keywords: Acoustic monitoring, Sampling design, Measurement uncertainty, Regulatory compliance, Spectral typology, Mixed-effects model

Posted Date: November 27th, 2026

DOI: https://doi.org/10.21203/rs.3.rs-11596023/v1

License: This work is licensed under a Creative Commons Attribution 4.0 International License.
Read Full License

Additional Declarations: No competing interests reported.

Octave-Band Characterisation of Heterogeneous Traffic Noise at Urban Intersections

Bhanu Chaudhary[1*], Bhaven N. Tandel[1], Manoranjan Parida[2]

[1] Department of Civil Engineering, Sardar Vallabhbhai National Institute of Technology, Surat 395007, Gujarat, India

[2] Department of Civil Engineering, Indian Institute of Technology Roorkee, Roorkee 247667, Uttarakhand, India

[*] Corresponding author: Bhanu Chaudhary, bhanuchaudhary40@gmail.com; ORCID 0000-0002-1152-3742

Abstract

Environmental noise monitoring in Indian cities relies on broadband A-weighted levels and on rating spectra derived from European traffic. This study assesses octave-band traffic noise at 15 signalised intersections in Surat, India, where two- and three-wheelers make up four-fifths of the fleet. A total of 203 half-hour records of L_{Aeq}, L_{max}, L_{min} and octave-band levels (31.5 Hz–8 kHz) were paired with video-classified traffic counts. Allowing for an expanded uncertainty of about 3 dB, 13 of the 15 sites exceeded their daytime limit conclusively. The normalised A-weighted spectrum peaked at 4 kHz in 76% of records; relative to ISO 717-1 Spectrum No. 2 it was 1.8–2.3 dB weaker at 125–250 Hz and 1.7 dB stronger at 2 kHz, and a median 41% of the A-weighted energy lay at 4–8 kHz, outside the rating range. Within an intersection, L_{Aeq} rose by only 0.18 dB per decibel of flow, against 0.95 dB between intersections. The high-frequency share was a stable site property, unrelated to flow or vehicle mix, and it divided the sites into three spectral types. A flow-and-composition model transferred poorly to unseen sites (leave-one-site-out error 3.8 dB; site biases up to 7.5 dB), whereas the local reference spectrum converted L_{Aeq} into 125 Hz–2 kHz band levels with errors of 0.6–1.6 dB, against 0.8–2.5 dB for the ISO spectrum. Seven half-hour windows were needed to fix a session level within ±1 dB. Site measurement, not flow-based prediction, should therefore anchor intersection assessment, supported by locally derived spectra.

Keywords Acoustic monitoring · Sampling design · Measurement uncertainty · Regulatory compliance · Spectral typology · Mixed-effects model

1 Introduction

Road traffic is the dominant source of environmental noise in cities, and long-term exposure is associated with annoyance, sleep disturbance and cardiovascular risk (Basner et al. 2014; World Health Organization Regional Office for Europe 2018) . In India, the problem is documented chiefly through monitoring. The National Ambient Noise Monitoring Network of the Central Pollution Control Board reports levels above the limits of the Noise Pollution (Regulation and Control) Rules at most stations in the major cities, year after year (N. Garg et al. 2016, 2017; Naveen Garg et al. 2017; Ministry of Environment and Forests 2000)and roadside surveys in Varanasi, Asansol and Delhi document the same pattern at street level (Banerjee et al. 2008; Mishra et al. 2010; Pathak et al. 2008) . Monitoring outputs, however, are almost always broadband A-weighted levels, and noise maps across the country are still produced without a normative framework adapted to local conditions (N. Garg et al. 2021) .

The prediction models on which assessment relies, including CoRTN, FHWA and RLS-90, were calibrated for homogeneous, lane-based traffic and perform poorly under Indian conditions (Naveen Garg and Maji 2014) . Horn use is a recurring explanation. Vijay et al. (Vijay et al. 2015) showed that honking raised roadside levels in Nagpur by 2–5 dB(A) and placed its energy in the 500 Hz, 2 kHz and 4 kHz octaves; Kalaiselvi and Ramachandraiah (Kalaiselvi and Ramachandraiah 2016) reported horn-related increments of 0.5–13 dB(A), and Thakre et al. (Thakre et al. 2020) introduced honking as an explicit predictor. In Surat, Sonaviya and Tandel (R. Sonaviya and N. Tandel 2021; Sonaviya and Tandel 2020) found only weak correlations between equivalent level and traffic volume, geometry or speed. Recent models developed for mid-sized Indian cities, at mid-block sections and at intersections, have turned to locally calibrated regression and neural-network forms (Chouksey et al. 2023; Yadav et al. 2024) . Signalised intersections add queuing, idling and acceleration, which alter both the level and the character of the noise (Can and Aumond 2018; Rajakumara and Mahalinge Gowda 2009) . Whether a model calibrated in one setting can be carried to another has been questioned even between developed countries (Peng et al. 2018) , and the question is sharper when the fleet itself differs.

Two monitoring questions follow directly. The first is how much measurement is needed. Studies of temporal sampling show that short records can estimate long-term levels only when their variability and stabilisation behaviour are known (Gaja et al. 2003; Prieto Gajardo and Barrigón Morillas 2015; Torija et al. 2011) , yet no such evidence exists for intersections carrying heterogeneous traffic, where the relation between level and flow is weak. The second

is what the measured noise contains. Free-flowing European traffic produces a spectrum dominated by tyre–road noise with a broad maximum near 1 kHz (Sandberg and Ejsmont 2002) , and the spectral emission terms of CNOSSOS-EU, Harmonoise and SonRoad are built on this fleet (ephalopoulos et al. 2012; Heutschi 2004; Jonasson 2007) . The spectrum responds to traffic dynamics (Can et al. 2010) , and spectral shape alters perceived loudness and annoyance at equal A-weighted level (Torija and Flindell 2014) ; two-wheeler noise is disproportionately annoying (Paviotti and Vogiatzis 2012) , while heavy vehicles add low-frequency content (Berglund et al. 1996) .

Spectral shape enters assessment practice directly. The adaptation term C_{tr} of ISO 717-1 weights the sound reduction index of façade elements by a standard urban traffic spectrum defined over 125 Hz–2 kHz in octave bands (International Organization for Standardization 2020) , and the single-number rating of noise barriers relies on the normalised traffic spectrum of EN 1793-3, which places its maximum weight at 1 kHz (European Committee for Standardization 1997) . The choice of these spectra was debated during the revision of ISO 717 on European evidence alone (Scholl et al. 2011) . No multi-site study has tested whether they represent heterogeneous Asian traffic, and noise mapping in Surat has so far relied on broadband indicators (Sonaviya and Tandel 2019) .

This study addresses both questions for signalised intersections in Surat, a fast-growing tier-II city in western India. It pursues five objectives: (i) to assess compliance with the national daytime limits while accounting for measurement uncertainty; (ii) to describe the temporal pattern of noise and traffic across the morning and evening peaks; (iii) to establish a reference octave-band spectrum for heterogeneous intersection traffic, compare it with ISO 717-1 Spectrum No. 2 and identify spectral site types; (iv) to determine whether level, noise floor, dynamic range and spectral balance follow traffic flow and composition, within and between intersections; and (v) to derive practical guidance for monitoring design, namely the number of half-hour windows required, the bias of single-window surveys, the transferability of flow-based prediction and the accuracy of spectral conversion from broadband levels.

2 Materials and methods

2.1 Study area and measurement sites

Surat, on the Tapi river in southern Gujarat, is among the fastest-growing cities in India. Fifteen signalised intersections, coded S1–S15, were selected to span the principal land-use categories

of the city: commercial (four sites), industrial (two), mixed (three), educational, recreational and residential (one each) and peri-urban (three). Twelve sites lie within the urban core and three on the peri-urban fringe. Eleven intersections have four approach arms, two have five, one has three and one has two (Table 1).

Table 1 Characteristics of the monitored intersections

Site	Land use	Arms	Windows	L_{Aeq} (dB(A))	PCU per 30 min	2W (%)	3W (%)	4W (%)	HV (%)
S1	Commercial	4	16	73.7	1087	56.0	31.7	8.0	2.6
S2	Commercial	4	16	68.6	1068	55.4	32.5	8.2	2.1
S3	Commercial	4	16	69.2	935	52.5	35.3	8.7	1.9
S4	Commercial	5	16	71.4	1060	55.0	33.0	8.1	2.2
S5	Educational	2	16	69.1	992	54.1	11.5	31.0	2.0
S6	Industrial	4	16	68.5	2606	55.2	13.2	18.9	12.4
S7	Industrial	4	16	76.7	2999	54.5	12.6	18.5	14.1
S8	Mixed	5	16	72.0	1154	58.2	29.7	9.9	1.0
S9	Mixed	4	16	71.8	989	57.0	30.9	9.5	1.5
S10	Mixed	3	16	71.2	1056	58.8	29.0	10.0	1.0
S11	Peri-urban	4	4	63.5	401	55.3	7.9	31.2	5.6
S12	Peri-urban	4	4	62.8	321	51.2	40.9	4.3	3.3
S13	Peri-urban	4	4	61.6	148	64.7	27.2	3.2	4.7
S14	Recreational	4	15	69.3	1307	69.1	20.5	9.5	0.6
S15	Residential	4	16	68.1	371	56.7	25.9	15.9	0.7

L_{Aeq} is the energy mean of the half-hour values; PCU is the mean flow per window. 2W two-wheelers, 3W three-wheelers (auto-rickshaws), 4W cars, HV heavy vehicles

2.2 Instrumentation and measurement procedure

Sound levels were recorded with a KIMO DB300/2 integrating sound level meter (KIMO Instruments, France; serial no. 17040239), a class 2 instrument conforming to IEC 61672-1 (International Electrotechnical Commission 2002) , with octave-band analysis from 31.5 Hz to 8 kHz (International Electrotechnical Commission 2014) . The meter had been calibrated by an accredited laboratory, and an acoustic calibrator was applied before each session. It was mounted on a tripod 1.5 m above the ground and 3 m from the kerb of the busiest approach, with a windscreen fitted and the microphone directed towards the carriageway (Fig. 1). Measurements followed ISO 1996-2 wherever site conditions permitted (International Organization for Standardization 2017) and were made in the first half of 2025 in dry weather with wind speeds below 5 m s^{-1}.

At each urban site, consecutive half-hour windows were recorded from 08:30 to 12:00 and from 17:30 to 21:00, spanning the morning and evening peaks. At the three peri-urban sites, four half-hour windows were distributed across the day. For every window the meter stored L_{Aeq}, L_{max}, L_{min} and unweighted equivalent levels in the nine octave bands from 31.5 Hz to 8

kHz. After screening for completeness and internal consistency, 203 windows were retained. The energetic sum of the A-weighted octave levels reproduced the measured L_{Aeq} to within −0.55 to +0.78 dB (5th–95th percentile; median 0.00 dB), confirming that broadband and spectral values describe the same record.



Fig. 1 Class 2 sound level meter mounted on a tripod at the kerbside of a monitored intersection in Surat

2.3 Traffic counts

Traffic was filmed throughout every measurement window and classified manually into two-wheelers (2W), three-wheelers (3W), cars (4W), heavy vehicles (HV), public transport buses (PT) and emergency vehicles. Counts were converted to passenger car units (PCU) with the equivalency factors recommended by the Indian Roads Congress; equivalency for mixed urban streams is itself flow-dependent (Dhamaniya and Chandra 2013) , so PCU is used here as an index of traffic intensity rather than of capacity. Emergency vehicles were retained in the PCU totals but excluded from composition shares, because their occurrence was intermittent.

2.4 Spectral descriptors

Each octave level L_j was A-weighted with the correction A_j of IEC 61672-1 and expressed relative to the overall A-weighted level of the window, so that the nine normalised bands sum energetically to 0 dB:

$$N_i = (L_i + A_i) - 10log_{10}\sum_{j=1}^{9} 10^{(L_j+A_j)/10} \quad (1)$$

Normalisation removes absolute level and isolates spectral shape. With the A-weighted band energy E_j defined as the term inside the sum of Eq. (1), three shape descriptors were derived. The high-frequency share is the fraction of A-weighted energy in the 4 and 8 kHz octaves,

$$S_{HF} = 100 \times \frac{E_{4k}+E_{8k}}{\sum_{j=1}^{9} E_j} \quad (2)$$

the spectral centroid is the energy-weighted geometric mean frequency,

$$f_c = exp\left(\frac{\sum_{j=1}^{9} E_j ln\, f_j}{\sum_{j=1}^{9} E_j}\right) \quad (3)$$

and the low-to-high balance compares the energy at or below 250 Hz with that at or above 2 kHz,

$$D_{LH} = 10log_{10}\sum_{j=1}^{4} E_j - 10log_{10}\sum_{j=7}^{9} E_j \quad (4)$$

The dominant band of a window is the octave with the highest A-weighted level. Traffic intensity was expressed as $Q = 10\ \log_{10}(\mathrm{PCU})$, so that a slope of 1.0 for any level corresponds to the 3 dB increase per doubling of flow assumed in energy-based emission models. The difference $L_{max} - L_{min}$ served as an index of the dynamic range of the noise.

2.5 Reference spectrum, principal components and spectral typology

For each site the median normalised level was computed in every band, and the reference spectrum was taken as the median of the 15 site medians. Treating the site rather than the window as the unit of analysis prevents the densely sampled urban sites from outweighing the peri-urban sites. Confidence intervals (95%) were obtained from 2000 bootstrap resamples of sites (Efron and Tibshirani 1993) . For comparison with ISO 717-1 Spectrum No. 2, the spectrum was renormalised over the octave rating range of the standard, 125 Hz–2 kHz (International Organization for Standardization 2020) . The structure of spectral variation was explored by principal component analysis of the centred matrix of normalised levels (203 windows × 9 bands) (Jolliffe and Cadima 2016) .

To test whether intersections fall into distinct spectral types, the 15 site-median spectra were grouped by agglomerative hierarchical clustering with Ward's minimum-variance criterion on Euclidean distances between normalised spectra (Ward 1963) . The number of types was chosen by the mean silhouette width over two to five clusters (Rousseeuw 1987) , and the resulting types were compared in flow, composition, level and dynamic range with the Kruskal–Wallis test.

2.6 Statistical modelling

Temporal patterns were described by the median and interquartile range of flow, L_{Aeq} and S_{HF} in each half-hour slot across the 12 urban sites. Morning and evening conditions were compared site by site with the Wilcoxon signed-rank test, and land-use groups with the Kruskal–Wallis test applied to site medians (Hollander et al. 2015) .

Because windows are nested within sites, ordinary regression would conflate differences between intersections with changes over time at a single intersection. Linear mixed-effects models with a random intercept for each site were therefore fitted, with traffic intensity decomposed into a between-site component (the site mean $\bar{Q}_s$) and a within-site component (the deviation from it) (Bell and Jones 2015) :

$$Y_{st} = \beta_0 + \beta_W\left(Q_{st} - \bar{Q}_s\right) + \beta_B \bar{Q}_s + \beta_P P_{st} + u_s + \varepsilon_{st} \tag{5}$$

Here Y_{st} is the outcome for window t at site s, P_{st} indicates the evening period, u_{s} N(0, σ^2^u) and $\varepsilon_{\mathrm{st}}$ N(0, σ^2_ε). The coefficient β_{W} measures how the outcome changes as flow varies at a given intersection, and β_{B} how it differs between intersections carrying different mean flows. Outcomes comprised L_{Aeq}, L_{max}, L_{min}, $L_{\mathrm{max}} - L_{\mathrm{min}}$, the A-weighted levels below and above 2 kHz, S_{HF}, f_{c} and each of the nine octave-band levels. A further model regressed S_{HF} on the within-site shares of 3W, 4W, HV and PT. Models were fitted by restricted maximum likelihood (Seabold and Perktold 2010) , and p-values within each family of tests were adjusted with the Benjamini–Hochberg procedure (Benjamini and Hochberg 1995) . The share of variance attributable to sites was expressed as the intraclass correlation (Koo and Li 2016) :

$$ICC = \frac{\sigma_u^2}{\sigma_u^2 + \sigma_\varepsilon^2} \tag{6}$$

2.7 Compliance assessment with measurement uncertainty

For each site the session level was the energy mean of its n_{s} half-hour values,

$$L_s = 10log_{10}\left(\frac{1}{n_s}\sum_{t=1}^{n_s} 10^{L_{st}/10}\right) \quad (7)$$

and its expanded uncertainty combined an instrumental and environmental component with the sampling component of the session (oint Committee for Guides in Metrology 2008) :

$$U_s = k\sqrt{u_{inst}^2 + \frac{s_s^2}{n_s}},\ k = 2 \quad (8)$$

where s_s is the standard deviation of the half-hour levels. A standard uncertainty u_{inst} = 1.5 dB was assigned to the class 2 instrument and the field conditions, in line with the values given for class 2 measurements in ISO 1996-2 (International Organization for Standardization 2017) . Session levels were compared with the daytime limits of the Noise Pollution Rules (Ministry of Environment and Forests 2000) : 65 dB(A) for commercial, mixed and recreational sites, 75 dB(A) for industrial sites and 55 dB(A) for residential and peri-urban sites. The educational site S5 was assessed against the residential limit, since no silence zone had been declared around it. Following the decision rules of JCGM 106 (Joint Committee for Guides in Metrology 2012) , a site was classed as exceeding its limit when $L_s - U_s$ was above the limit, as complying when $L_s + U_s$ was below it, and as indeterminate otherwise. The session covers the two daily peaks rather than the full 06:00–22:00 period, so L_s is an indicator of peak-period daytime exposure rather than a statutory daytime level.

2.8 Monitoring design and transferability

Four analyses addressed monitoring practice. (i) *Sampling adequacy*: at each urban site, k = 1–12 windows were drawn at random without replacement 500 times, and the 95th percentile of the absolute error of the subsample against the full-session value was recorded for L_s, the median S_{HF} and the largest deviation of any normalised band from the site-median spectrum (Gaja et al. 2003; Prieto Gajardo and Barrigón Morillas 2015) . (ii) *Single-window representativeness*: the error of each half-hour slot as a stand-alone estimate of L_s was summarised by its mean (bias) and root-mean-square error across the 12 urban sites. (iii) *Transferability of flow-based prediction*: an ordinary least-squares model of L_{Aeq} on Q, the HV and 3W shares and the evening indicator was fitted with each site left out in turn and used to predict the omitted site (leave-one-site-out, LOSO). (iv) *Spectral conversion*: A-weighted band levels at each omitted site were predicted from its measured L_{Aeq} and the reference spectrum of the remaining 14 sites,

$$L_{A,i} = L_{Aeq} + N_i^{ref} \quad (9)$$

and, over 125 Hz–2 kHz, the same prediction was repeated with ISO 717-1 Spectrum No. 2 in place of the local spectrum, both renormalised over that range. Errors were summarised as LOSO root-mean-square error (RMSE) per band.

2.9 Consequence for spectrum-adapted ratings

The A-weighted level reduction delivered by a building element with sound reduction index R_i against a normalised source spectrum L_i is

$$X_A = -10log_{10} \sum_i 10^{(L_i - R_i)/10} \quad (10)$$

and the ISO 717-1 adaptation term equals X_A minus the weighted sound reduction index. X_A was evaluated for three generic transmission-loss curves, representing a mass-law element rising 6 dB per octave, single glazing with a coincidence dip at 2 kHz and a double-leaf element, with both the ISO spectrum and the measured spectrum. The curves are illustrative and do not describe specific products. All analyses were run in Python with statsmodels, SciPy and scikit-learn.

3 Results

3.1 Descriptive statistics

Table 2 summarises the 203 windows. Half-hour L_{Aeq} ranged from 60.5 to 79.1 dB(A) (median 69.9 dB(A)), with maxima reaching 97.7 dB(A) and minima as low as 38.2 dB(A) at the peri-urban sites. The median dynamic range, $L_{max} - L_{min}$, was 29.2 dB. Flow averaged 1242 PCU per half hour and varied more than forty-fold between the quietest peri-urban window and the busiest industrial one. Two-wheelers made up 56.8% of all vehicles, three-wheelers 22.9%, cars 13.9%, heavy vehicles 5.4% and buses 0.9%; the two industrial sites carried by far the largest heavy-vehicle shares (12.8% and 14.1%).

Table 2 Descriptive statistics of acoustic and traffic variables (203 half-hour windows, 15 sites)

Variable	Unit	Mean	SD	Min	Median	Max
L_{Aeq}	dB(A)	70.1	3.3	60.5	69.9	79.1
L_{max}	dB(A)	87.5	4.9	70.5	87.4	97.7
L_{min}	dB(A)	57.4	6.2	38.2	58.1	64.8
$L_{max} - L_{min}$	dB	30.1	6.7	5.7	29.2	51.4
Traffic flow	PCU/30 min	1242	863	104	1097	4408
All vehicles	veh/30 min	1482	942	137	1336	4814
Two-wheelers	veh/30 min	842	542	97	725	2747
Three-wheelers	veh/30 min	339	188	31	303	905
Cars	veh/30 min	206	199	1	126	867
Heavy vehicles	veh/30 min	80	160	1	21	672

Variable	Unit	Mean	SD	Min	Median	Max
Buses	veh/30 min	14	11	0	10	65
S_{HF}	%	40.5	12.7	9.4	40.8	70.0
Spectral centroid f_c	Hz	1785	370	736	1756	2800
D_{LH}	dB	−10.5	2.2	−14.6	−10.6	−0.7

S_{HF} share of A-weighted energy in the 4 and 8 kHz octaves; D_{LH} A-weighted level at or below 250 Hz minus that at or above 2 kHz

3.2 Compliance with daytime limits

Exceedance was the norm (Table 3, Fig. 2). Of the 203 windows, 89.7% exceeded the daytime limit of their zone, by a median 5.9 dB (90th percentile 12.3 dB); every urban window at the commercial, mixed and recreational sites exceeded 65 dB(A), and every window at the residential and peri-urban sites exceeded 55 dB(A). The expanded uncertainty of the session level was 3.0–3.3 dB at every site and was dominated by the instrumental component; the sampling component did not exceed 0.65 dB even at the peri-urban sites with four windows. Thirteen sites exceeded their limit by more than U_s, so that their non-compliance is established beyond reasonable measurement doubt. The two industrial sites behaved differently: S6 lay 6.5 dB below the industrial limit and complied conclusively, whereas S7 exceeded it by 1.7 dB, a margin within its uncertainty. The largest margins occurred where the limit is strictest: 14.1 dB at the educational site S5 and 13.1 dB at the residential site S15. Had S5 been formally declared a silence zone, the margin would have risen by a further 5 dB.

Median levels ranged from 62.7 dB(A) at the peri-urban sites to 72.2 dB(A) at the industrial sites, but differences between land-use groups represented by more than one site were not significant (Kruskal–Wallis $p = 0.10$). Land use therefore sets the limit, not the level: intersections in residential and educational settings carried noise of the same order as commercial ones and failed their stricter limits by the widest margins.

Table 3 Session levels, expanded uncertainty and compliance with the daytime limits of the Noise Pollution (Regulation and Control) Rules

Site	Land use	Limit (dB(A))	n_s	L_s (dB(A))	s_s (dB)	U_s (dB)	L_s − limit (dB)	Decision
S1	Commercial	65	16	73.7	1.15	3.05	+8.7	Exceeds
S2	Commercial	65	16	68.6	0.86	3.03	+3.6	Exceeds
S3	Commercial	65	16	69.2	1.76	3.13	+4.2	Exceeds
S4	Commercial	65	16	71.4	1.03	3.04	+6.4	Exceeds
S5	Educational	55[a]	16	69.1	2.40	3.23	+14.1	Exceeds
S6	Industrial	75	16	68.5	1.16	3.06	−6.5	Complies
S7	Industrial	75	16	76.7	1.77	3.13	+1.7	Indeterminate
S8	Mixed	65	16	72.0	0.89	3.03	+7.0	Exceeds
S9	Mixed	65	16	71.8	2.58	3.27	+6.8	Exceeds
S10	Mixed	65	16	71.2	0.95	3.04	+6.2	Exceeds

Site	Land use	Limit (dB(A))	n_s	L_s (dB(A))	s_s (dB)	U_s (dB)	L_s − limit (dB)	Decision
S11	Peri-urban	55	4	63.5	0.90	3.13	+8.5	Exceeds
S12	Peri-urban	55	4	62.8	0.31	3.02	+7.8	Exceeds
S13	Peri-urban	55	4	61.6	1.00	3.16	+6.6	Exceeds
S14	Recreational	65	15	69.3	1.09	3.05	+4.3	Exceeds
S15	Residential	55	16	68.1	0.85	3.03	+13.1	Exceeds

U_s expanded uncertainty ($k = 2$) with $u_{inst} = 1.5$ dB. Decision rule: exceeds if $L_s - U_s >$ limit; complies if $L_s + U_s <$ limit; indeterminate otherwise. [a] Residential limit; 50 dB(A) would apply if a silence zone were declared

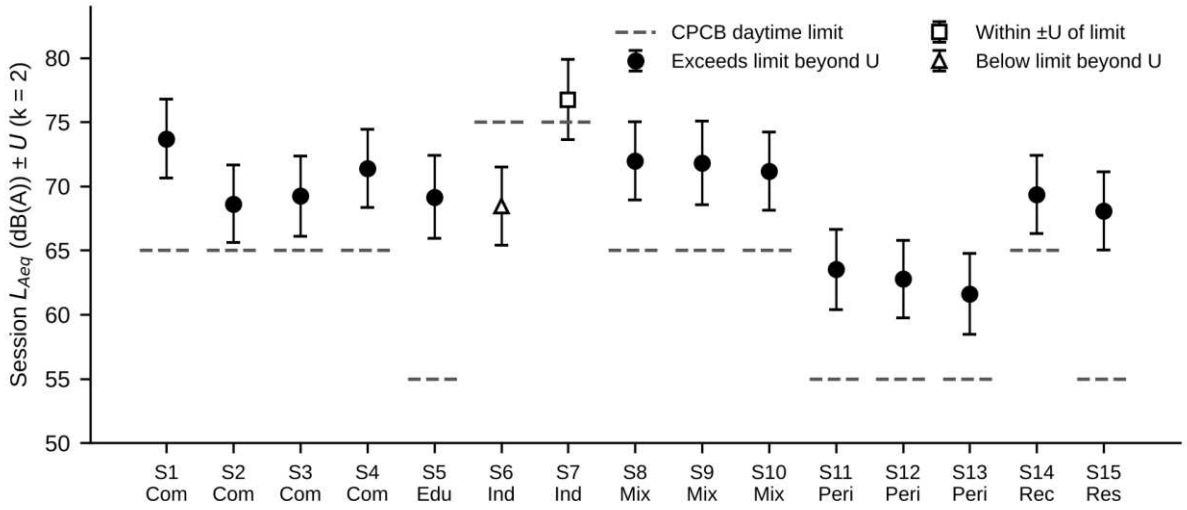

Fig. 2 Session L_{Aeq} at each site with its expanded uncertainty ($k = 2$) against the applicable daytime limit. Filled circles: exceedance beyond the uncertainty; open square: within ±U of the limit; open triangle: compliance beyond the uncertainty

3.3 Temporal pattern of traffic and noise

Traffic at the urban sites followed a pronounced diurnal cycle (Fig. 3a). Median flow rose to 1765 PCU per half hour at 10:00, fell to about 740 PCU by late morning, recovered to 1340 PCU between 18:30 and 19:30 and dropped sharply to 516 PCU at 20:00. The morning peak dominated: at 10 of the 12 urban sites the busiest half hour fell between 08:30 and 10:00, and the peak half hour carried a median 1.5 times the site mean flow (range 1.35–2.05). Composition was comparatively steady (Fig. 3c), although three-wheelers formed a larger share in the evening.

Noise did not follow this cycle. Median L_{Aeq} stayed between 68.8 and 71.6 dB(A) in every slot (Fig. 3b), so a 3.4-fold swing in flow, equivalent to 5.3 dB in Q, produced a spread of only 2.8 dB in level. At individual sites the contrast was sharper still: between the busiest and quietest half hours flow differed by a median 5.5 dB in Q but L_{Aeq} by only 1.2 dB, and at four sites the busiest half hour was no more than 0.1 dB louder than the quietest. The high-frequency share

moved independently of flow and reached its highest values in the lightly trafficked late-evening slots (45.6–47.5% at 20:00–20:30).

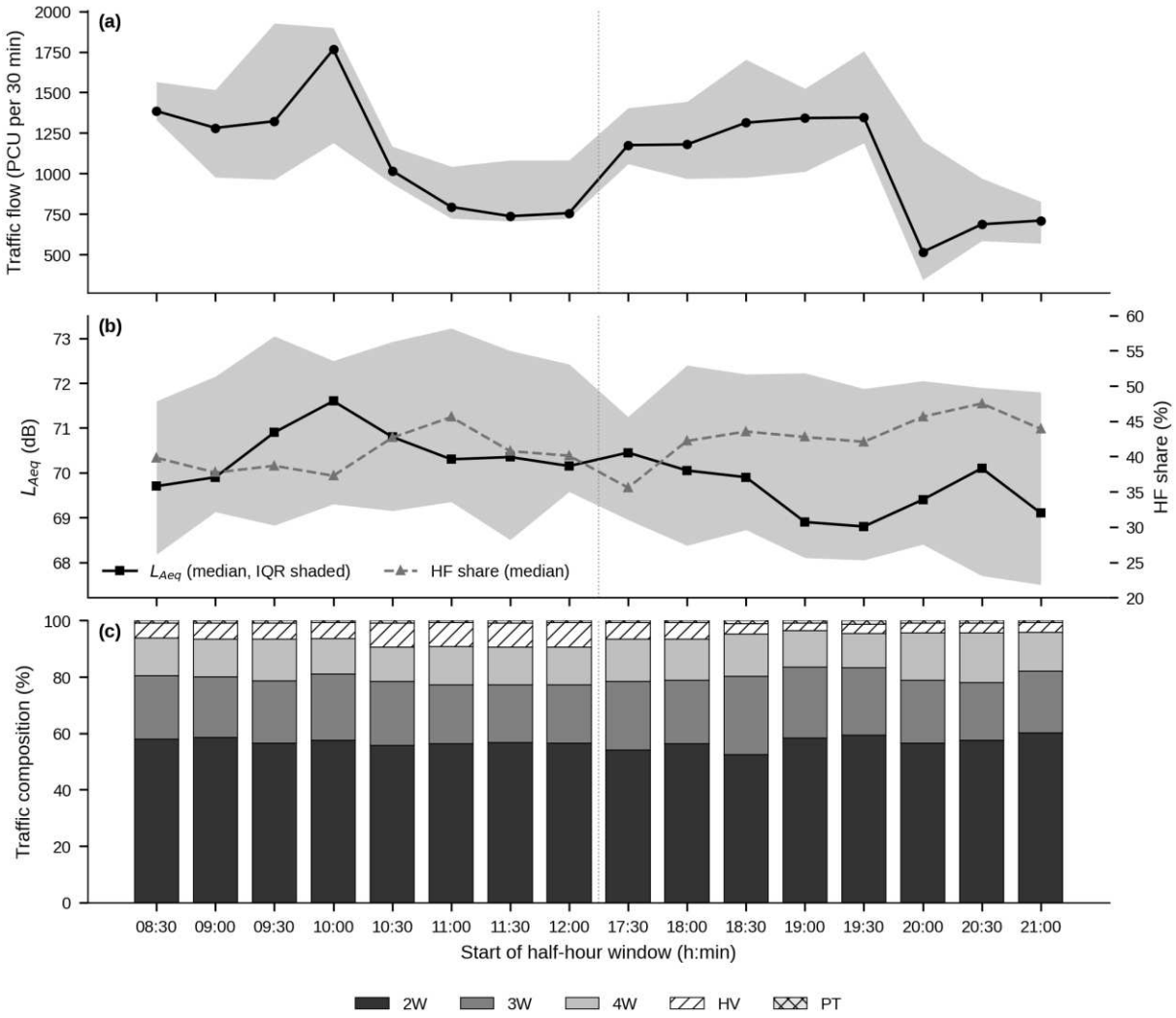

Fig. 3 Diurnal pattern at the 12 urban sites: (a) traffic flow, (b) L_{Aeq} and high-frequency share, (c) traffic composition. Lines show medians and shading the interquartile range; the dotted line separates the morning and evening sessions

Table 4 compares the two sessions site by site. None of the differences in level, dynamic range, flow or spectral shape reached significance after correction for multiple testing. The heavy-vehicle share was lower in the evening (median 1.6% against 2.5%, unadjusted $p = 0.035$) and the three-wheeler share higher (29.5% against 25.2%, $p = 0.083$), but neither difference survived adjustment. Once flow was controlled in the mixed-effects models (Sect. 3.7), evening L_{Aeq} was 0.53 dB lower ($p = 0.008$) and L_{min} 1.18 dB lower ($p = 0.010$), indicating a slightly quieter background at equal flow after dark.

Table 4 Morning and evening conditions compared site by site (medians over 15 sites; Wilcoxon signed-rank test)

Variable	Morning	Evening	Median difference	p	p_{BH}
L_{Aeq} (dB(A))	69.8	68.7	−0.3	0.252	0.466
L_{max} (dB(A))	87.7	85.0	−0.7	0.229	0.466
L_{min} (dB(A))	58.0	56.3	−0.3	0.272	0.466
$L_{max} - L_{min}$ (dB)	28.9	30.7	−0.1	0.826	0.901
Flow (PCU/30 min)	1084	979	−63	0.229	0.466
2W share (%)	57.0	56.0	−0.6	0.229	0.466
3W share (%)	25.2	29.5	+1.5	0.083	0.466
4W share (%)	10.5	9.4	−0.6	0.804	0.901
HV share (%)	2.5	1.6	−0.2	0.035	0.424
PT share (%)	1.0	1.1	+0.0	0.730	0.901
S_{HF} (%)	36.4	35.7	+1.1	0.359	0.539
Spectral centroid (Hz)	1720	1655	+6	0.978	0.978

Levels are energy means per site and session; shares are computed from pooled counts. p_{BH} Benjamini–Hochberg adjusted

3.4 Reference octave-band spectrum

The normalised A-weighted spectrum was strikingly consistent from site to site (Fig. 4a). Between-site standard deviations were only 0.7–1.6 dB per band, and within-site standard deviations 0.6–1.8 dB (Table 5). The reference spectrum rises steeply to 1 kHz, levels off between 1 and 2 kHz and reaches its maximum in the 4 kHz band (−5.0 dB; 95% CI −5.8 to −3.3 dB) before falling to −14.8 dB at 8 kHz. The 4 kHz band was the loudest A-weighted band in 76.4% of windows and at 12 of the 15 sites; the 1 kHz band dominated in 19.2% of windows and the 2 kHz band in 3.9%.

Table 5 Normalised A-weighted octave-band reference spectrum and unweighted band levels

Band (Hz)	Reference (dB)	95% CI (dB)	Between-site SD (dB)	Within-site SD (dB)	Unweighted median (dB)	Unweighted IQR (dB)
31.5	−46.0	−46.5 to −45.3	1.3	1.5	64.4	62.1–65.9
63	−28.8	−29.5 to −27.8	1.1	1.8	67.6	65.9–70.2
125	−18.4	−19.0 to −18.0	1.1	1.3	67.4	65.9–69.8
250	−13.9	−14.9 to −13.4	1.3	1.0	64.2	62.7–66.3
500	−9.5	−10.5 to −9.1	1.1	1.2	64.0	61.7–65.5
1000	−6.4	−7.7 to −6.0	1.1	0.9	63.2	61.4–65.2
2000	−6.7	−6.9 to −6.2	0.7	0.6	61.8	60.1–64.2
4000	−5.0	−5.8 to −3.3	1.6	1.2	64.2	62.0–67.4
8000	−14.8	−15.8 to −13.9	1.3	1.4	55.3	53.5–58.5

Reference = median of site medians; CI from 2000 bootstrap resamples of sites. Unweighted values are absolute band levels over all windows

In unweighted terms the highest levels occurred at 63 and 125 Hz (medians 67.6 and 67.4 dB), as expected for traffic noise. Above 250 Hz, however, the unweighted spectrum fell to 61.8 dB at 2 kHz and then climbed again to 64.2 dB at 4 kHz (Fig. 4b). Tyre–road dominated traffic

noise shows no such secondary maximum; its level declines steadily above about 1 kHz (Sandberg and Ejsmont 2002) .

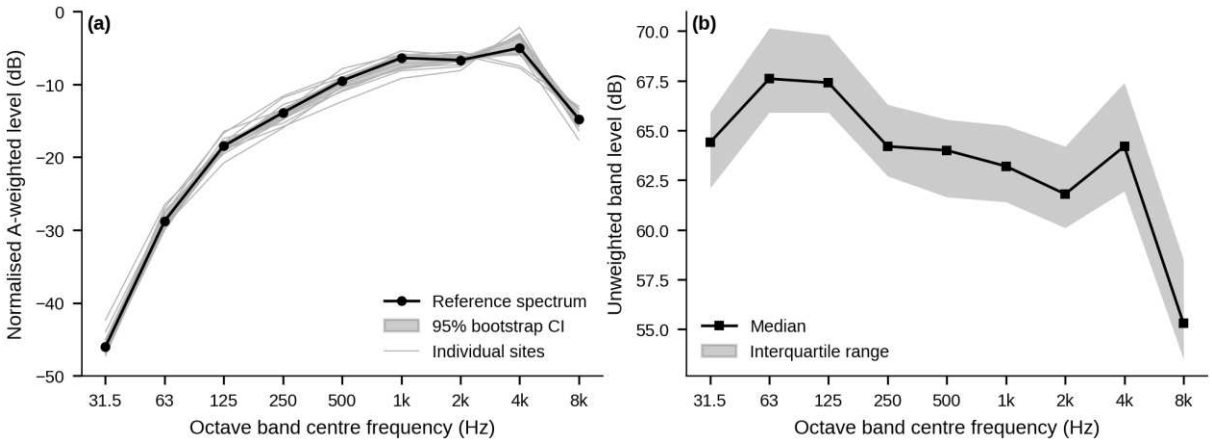

Fig. 4 (a) Normalised A-weighted spectra of the 15 sites, the reference spectrum and its 95% bootstrap confidence interval; (b) median and interquartile range of unweighted octave-band levels

3.5 Comparison with ISO 717-1 and distribution of energy

Over the 125 Hz–2 kHz rating range the measured spectrum departed systematically from ISO 717-1 Spectrum No. 2 (Table 6, Fig. 5). It was 2.3 dB weaker at 125 Hz and 1.8 dB weaker at 250 Hz, close to the standard at 500 Hz and 1 kHz, and 1.7 dB stronger at 2 kHz. None of the confidence intervals contained the ISO value. Heterogeneous intersection traffic is therefore less weighted towards low frequencies, and more towards high frequencies, than the traffic assumed in C_{tr}.

Table 6 Measured spectrum and ISO 717-1 Spectrum No. 2, both normalised to 0 dB over 125 Hz–2 kHz

Band (Hz)	Present study (dB)	95% CI (dB)	ISO 717-1 Sp. 2 (dB)	Difference (dB)
125	−16.3	−16.8 to −16.0	−14	−2.3
250	−11.8	−12.1 to −11.5	−10	−1.8
500	−7.5	−7.7 to −7.1	−7	−0.5
1000	−4.6	−4.7 to −4.3	−4	−0.6
2000	−4.3	−4.7 to −4.0	−6	+1.7

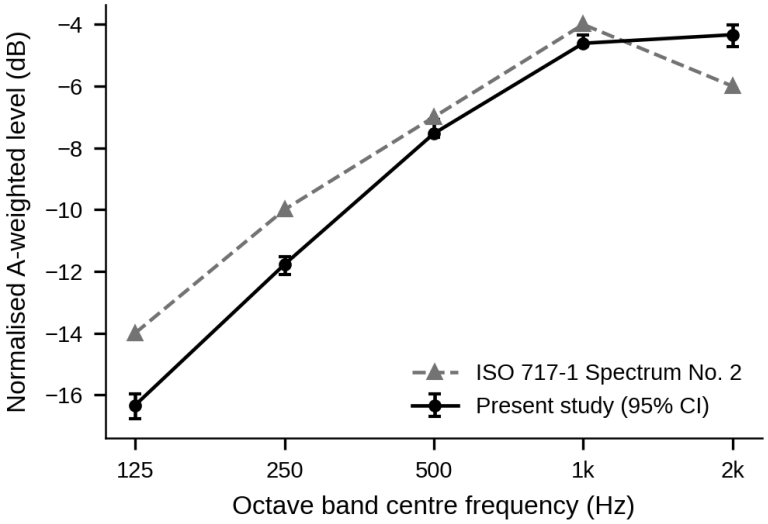

Fig. 5 Measured A-weighted spectrum (95% CI) compared with ISO 717-1 Spectrum No. 2 over the octave rating range

The 4 kHz maximum places a large part of the A-weighted energy above the octave range of the standard (Table 7). The 4 and 8 kHz bands together carried a median 40.8% of the energy per window (interquartile range 32.5–49.1%), almost all of it at 4 kHz, while bands below 125 Hz contributed a negligible 0.1%. The share differed markedly between sites, from 21.1% at S5 to 62.8% at S7 (Fig. 6), and 60% of its variance lay between sites (ICC = 0.60).

Table 7 Distribution of A-weighted energy across frequency ranges (203 windows)

Frequency range	Median share (%)	Interquartile range (%)
31.5–63 Hz	0.1	0.1–0.2
125 Hz–2 kHz (ISO 717-1 octave rating range)	59.1	50.8–67.3
4 kHz	37.0	28.4–46.8
8 kHz	2.8	2.3–4.1
4–8 kHz (outside the rating range)	40.8	32.5–49.1

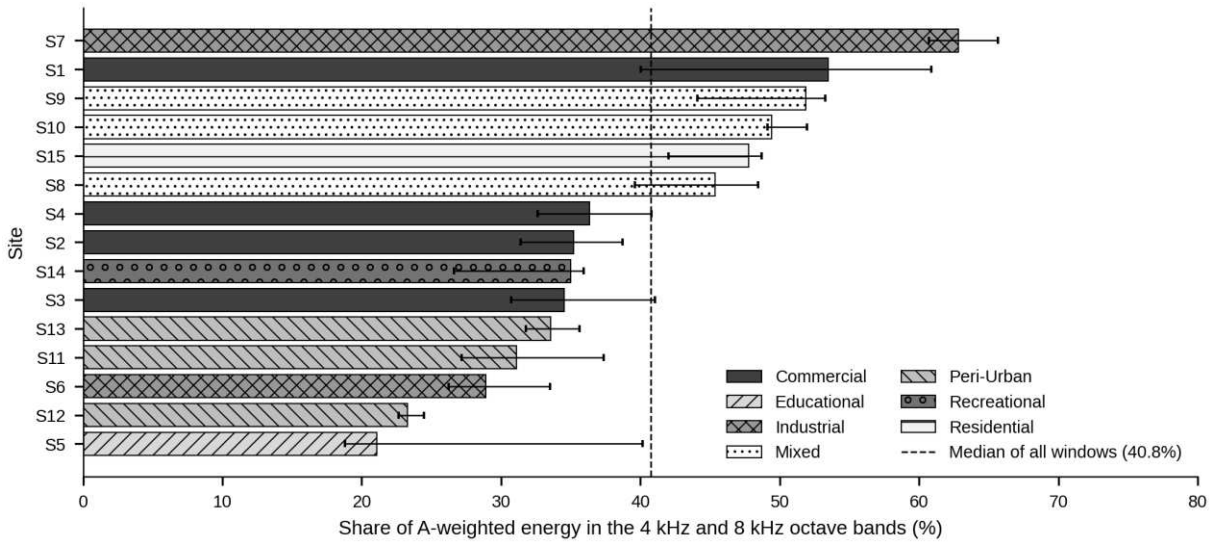

Fig. 6 Median share of A-weighted energy in the 4 and 8 kHz octaves at each site, with interquartile ranges, grouped by land use

3.6 Principal components and spectral site types

Principal component analysis confirmed that the high-frequency balance is the principal axis along which spectra differ (Fig. 7). The first component explained 51.5% of the variance in normalised spectra; it loaded positively on the 4 kHz band and negatively on all bands from 31.5 Hz to 1 kHz, and its scores correlated strongly with S_{HF} (r = 0.82). The second component (16.1%) contrasted the lowest two bands and 4 kHz with the mid-frequency bands.

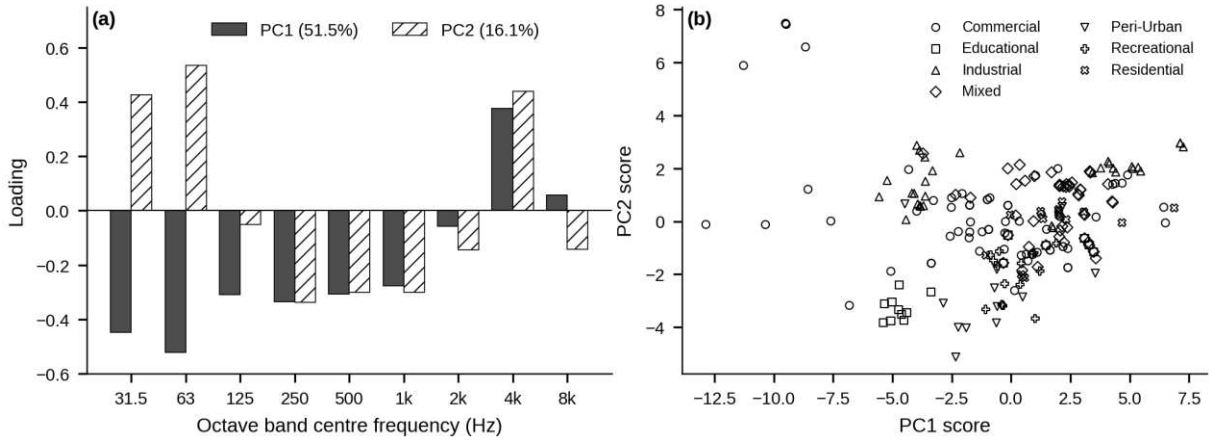

Fig. 7 Principal component analysis of normalised A-weighted spectra: (a) loadings of the first two components; (b) window scores by land use

Hierarchical clustering of the site spectra gave the highest mean silhouette width for three types (0.35, against 0.34 for two and 0.31 for four), and the dendrogram separated one well-defined group from the rest at the largest linkage distance (Fig. 8a). Type 1 (S1, S7, S8, S9, S10, S15) has a pronounced 4 kHz peak, a high-frequency share of 51.8% and a centroid near 2.1 kHz. Type 2 (S2, S3, S6) is richer in low frequencies, about 2.5 dB stronger at 31.5 Hz than the other

types, with a smaller 4 kHz peak. Type 3 (S4, S5, S11–S14) is nearly flat from 1 to 4 kHz and has the lowest high-frequency share (30.1%) (Table 8, Fig. 8b). The types are not proxies for traffic: they did not differ in flow, three-wheeler, car or heavy-vehicle share or dynamic range (all $p \geq 0.36$), and differed only marginally in level ($p = 0.06$). Nor do they follow land use, since Type 1 contains commercial, industrial, mixed and residential sites. The spectral character of an intersection is thus a property of the site itself.

Table 8 Spectral site types identified by Ward clustering of site-median normalised spectra

Type	Sites	S_{HF} (%)	f_c (Hz)	$N_{31.5}$ (dB)	N_{4k} (dB)	L_s (dB(A))	PCU/30 min	3W (%)	HV (%)
1	S1, S7, S8, S9, S10, S15	51.8	2095	−46.3	−3.1	72.2	1276	26.6	3.6
2	S2, S3, S6	32.9	1538	−43.8	−5.2	68.8	1536	26.9	5.6
3	S4, S5, S11, S12, S13, S14	30.1	1550	−46.2	−6.2	66.3	705	23.3	3.1
p (Kruskal–Wallis)						0.06	0.36	0.66	0.56

Values are means of site values within each type. $N_{31.5}$ and N_{4k} normalised A-weighted levels in the 31.5 Hz and 4 kHz bands

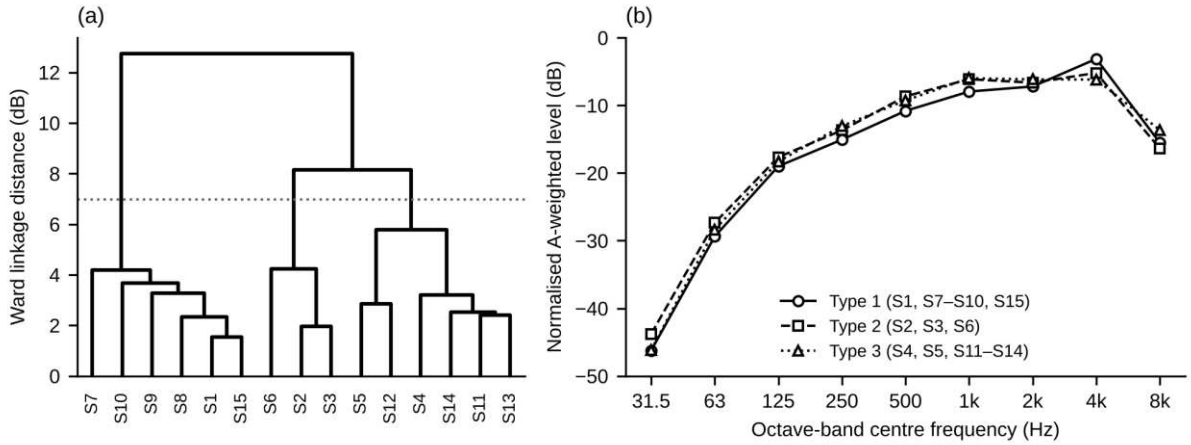

Fig. 8 Spectral site types: (a) Ward dendrogram of site-median normalised spectra, with the three-type cut shown dotted; (b) mean normalised A-weighted spectrum of each type

3.7 Dependence on traffic flow and composition

Table 9 presents the mixed-effects estimates. Between sites, L_{Aeq} increased by 0.95 dB per decibel of Q (95% CI 0.56–1.35), consistent with the energy relation. Within sites the slope collapsed to 0.18 (0.04–0.31), or about 0.5 dB per doubling of flow (Fig. 9b). Most of the variance in L_{Aeq} lay between sites (ICC = 0.88).

Table 9 Within-site and between-site effects of traffic intensity Q on level and spectral descriptors (linear mixed-effects models; 203 windows, 15 sites)

Outcome	Within-site slope (95% CI)	p_{BH}	Between-site slope (95% CI)	p	Evening effect (p)	ICC
L_{Aeq}	0.18 (0.04, 0.31)	0.036	0.95 (0.56, 1.35)	<0.001	−0.53 (0.008)	0.88

Outcome	Within-site slope (95% CI)	p_{BH}	Between-site slope (95% CI)	p	Evening effect (p)	ICC
L_{max}	−0.04 (−0.39, 0.32)	0.841	0.49 (−0.02, 1.00)	0.057	−0.84 (0.125)	0.40
L_{min}	0.31 (0.01, 0.61)	0.092	2.01 (1.24, 2.79)	<0.001	−1.18 (0.010)	0.86
$L_{max} - L_{min}$	−0.34 (−0.79, 0.10)	0.212	−1.49 (−2.30, −0.68)	<0.001	+0.34 (0.618)	0.66
L_A, 31.5 Hz–2 kHz	0.19 (0.07, 0.31)	0.019	0.86 (0.56, 1.17)	<0.001	−0.63 (<0.001)	0.86
L_A, 4–8 kHz	0.21 (0.01, 0.41)	0.092	1.06 (0.52, 1.61)	<0.001	−0.37 (0.218)	0.83
S_{HF} (%)	0.10 (−0.66, 0.87)	0.841	1.08 (−0.52, 2.69)	0.186	+1.50 (0.198)	0.60
f_c (Hz)	9.2 (−14.1, 32.5)	0.586	21.6 (−24.5, 67.6)	0.358	+35.7 (0.316)	0.55

Slopes for levels in dB per dB of $Q = 10 \log_{10}(\text{PCU})$; for S_{HF} in percentage points; for f_c in Hz. Evening effect is the adjusted difference from the morning session. p_{BH} Benjamini–Hochberg adjusted across the within-site tests

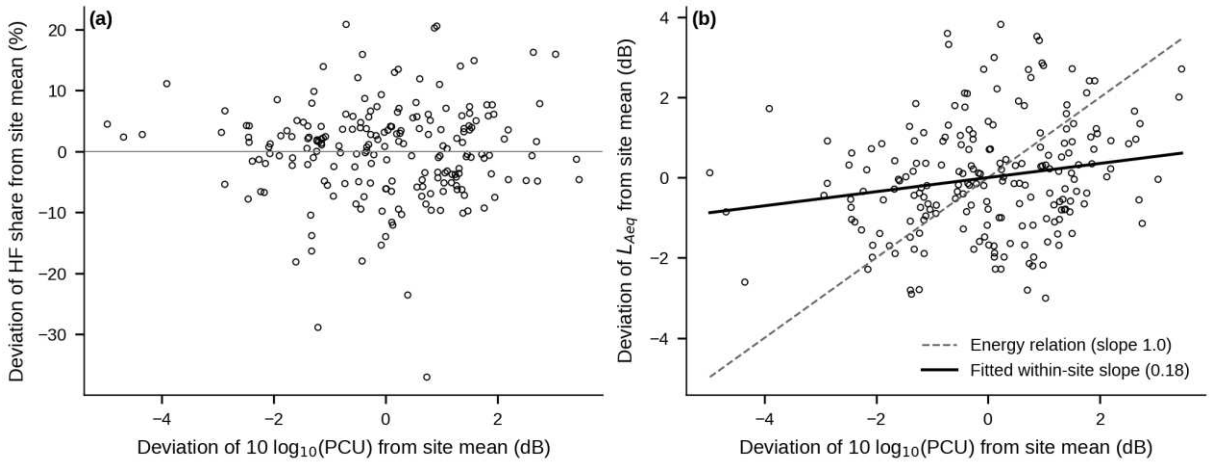

Fig. 9 Within-site deviations of (a) high-frequency share and (b) L_{Aeq} against within-site deviations of traffic intensity. In (b) the dashed line shows the energy relation and the solid line the fitted within-site slope

The decoupling held across the entire spectrum. When each octave band was modelled separately, within-site slopes lay between 0.15 and 0.29 in every band from 31.5 Hz to 8 kHz, whereas between-site slopes ranged from 0.64 to 1.13 (Table 10, Fig. 10). No frequency band responded to changes in flow at a given intersection in the manner assumed by emission models.

Table 10 Band-wise within-site and between-site slopes of octave-band level on traffic intensity, and site share of variance in normalised band level

Band (Hz)	Within-site slope (95% CI)	p_{BH}	Between-site slope (95% CI)	p	ICC of N_i
31.5	0.19 (0.03, 0.36)	0.035	1.05 (0.71, 1.40)	<0.001	0.44
63	0.25 (0.04, 0.46)	0.035	1.06 (0.71, 1.41)	<0.001	0.32
125	0.23 (0.07, 0.38)	0.013	0.97 (0.59, 1.34)	<0.001	0.35
250	0.17 (0.04, 0.30)	0.026	0.77 (0.47, 1.07)	<0.001	0.56
500	0.16 (−0.00, 0.32)	0.056	0.93 (0.62, 1.24)	<0.001	0.33
1000	0.15 (0.01, 0.28)	0.041	0.87 (0.58, 1.16)	<0.001	0.57
2000	0.25 (0.12, 0.38)	0.001	0.82 (0.49, 1.15)	<0.001	0.54
4000	0.20 (−0.00, 0.41)	0.056	1.13 (0.56, 1.70)	<0.001	0.54
8000	0.29 (0.11, 0.47)	0.008	0.64 (0.22, 1.06)	0.003	0.45

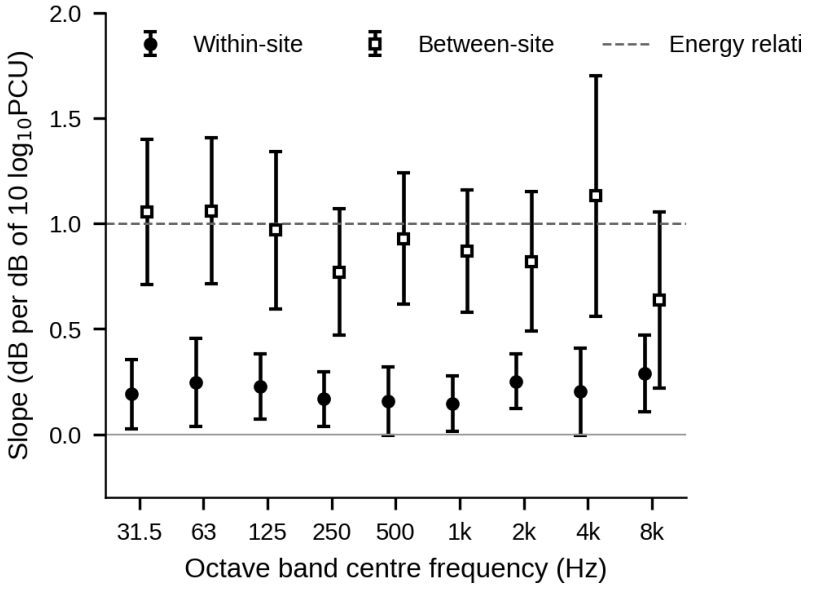

Fig. 10 Within-site and between-site slopes of octave-band level on 10 $\log_{10}$(PCU), with 95% confidence intervals. The dashed line marks the energy relation

Flow reshaped the statistical distribution of the noise rather than its peaks. Between sites, L_{min} rose by 2.01 dB per decibel of Q (1.24–2.79), twice the rate implied by the energy relation, whereas L_{max} rose by only 0.49 dB ($p = 0.057$). The dynamic range therefore contracted by 1.49 dB per decibel of Q (Fig. 11). Busier intersections were not markedly louder at their peaks; instead the quiet gaps between vehicles filled in, and the noise became steadier.

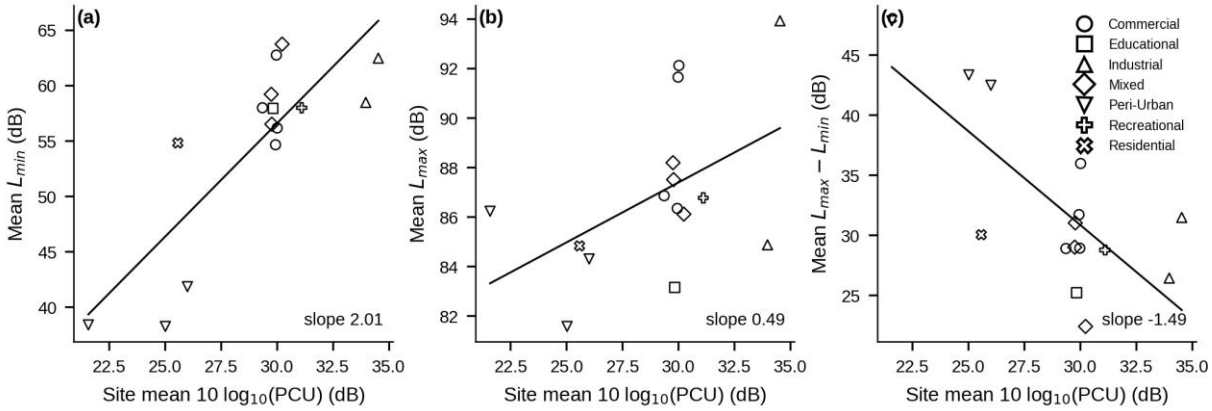

Fig. 11 Site mean (a) L_{min}, (b) L_{max} and (c) $L_{max} - L_{min}$ against site mean traffic intensity. Lines are least-squares fits; slopes are the between-site estimates of Table 9

Spectral shape showed no dependence on traffic at either level. Within sites, the correlation between Q and S_{HF} was 0.00 (Fig. 9a), and neither S_{HF} nor f_c responded to flow within or between sites (all $p \geq 0.19$). None of the within-site vehicle shares predicted S_{HF} (3W, 4W, HV and PT; all adjusted $p > 0.67$), and pooled rank correlations between composition and S_{HF} did not exceed 0.07 in magnitude (Appendix Table A2). Yet within a site L_{Aeq} tracked the 4–8 kHz

level closely (r = 0.84), almost as closely as it tracked the level below 2 kHz (r = 0.90). The high-frequency component therefore moves the overall level without being driven by the number or type of vehicles.

3.8 Implications for monitoring design

How many windows are needed. The error of a short survey fell steadily with the number of half-hour windows (Table 11, Fig. 12a). A single window estimated the session level within 2.9 dB in 95% of cases; three windows brought this to 1.7 dB, and seven windows (3.5 h) were needed to stay within ±1 dB. Spectral descriptors converged more slowly. The high-frequency share required 11 windows to fall within ±5 percentage points, and the largest error in any normalised band was still 1.2 dB with 12 windows. Because the windows are drawn from a 16-window session, the errors for large k describe agreement with that session and are optimistic as estimates of longer-term levels.

Table 11 Sampling error of short surveys at the 12 urban sites (95th percentile of absolute error against the full session; 500 random draws per site)

Windows k	Duration (h)	L_s (dB)	S_{HF} (percentage points)	Largest band error, N_i (dB)
1	0.5	2.90	18.5	5.44
2	1.0	2.37	13.5	4.14
3	1.5	1.73	12.0	2.91
4	2.0	1.39	9.4	2.59
6	3.0	1.02	8.0	1.95
7	3.5	0.86	7.7	1.97
8	4.0	0.80	6.0	1.65
10	5.0	0.61	5.4	1.37
11	5.5	0.53	4.4	1.41
12	6.0	0.44	3.5	1.21

When to measure. Single windows were least biased in the morning (Fig. 12b). The 10:30 window had the smallest RMSE (1.08 dB), while windows after 19:00 understated the session level by 0.5–1.05 dB, with RMSE up to 1.89 dB at 20:30. A one-off survey in the late evening, when traffic is light, will therefore underestimate peak-period exposure even though level varies little through the day.

Whether level can be predicted from traffic. A pooled model of L_{Aeq} on flow, heavy-vehicle and three-wheeler shares and period explained 33% of the variance ($R^2 = 0.33$), with flow the only clear predictor (0.66 dB per dB of Q). Applied to sites it had not seen, it performed poorly: the LOSO RMSE was 3.78 dB (mean absolute error 2.97 dB), 41.4% of windows were mispredicted by more than 3 dB, and the error was dominated by site-level bias (Fig. 12c). The model overpredicted the busy but comparatively quiet industrial site S6 by 6.5 dB and

underpredicted S7 by 7.5 dB; six sites carried biases larger than 3 dB. For comparison, the within-site standard deviation of half-hour levels was 1.38 dB. Two half-hour measurements at a site therefore estimate its level better than a flow-based prediction calibrated on 14 other intersections.

Whether spectra can be inferred from broadband levels. The reference spectrum transferred well. Predicting A-weighted band levels of an omitted site from its L_{Aeq} and the reference spectrum of the other 14 sites gave RMSE of 0.9–2.4 dB across the nine bands, and 0.9 dB at 2 kHz. Over 125 Hz–2 kHz the local spectrum gave 0.58–1.59 dB, against 0.78–2.52 dB for ISO 717-1 Spectrum No. 2 (Fig. 12d), which overpredicted the 125 and 250 Hz bands by about 2 dB and underpredicted 2 kHz by 1.5 dB. Where only broadband data exist, as in most Indian monitoring, the local spectrum provides band levels about as accurately as a single half-hour measurement provides the session level.

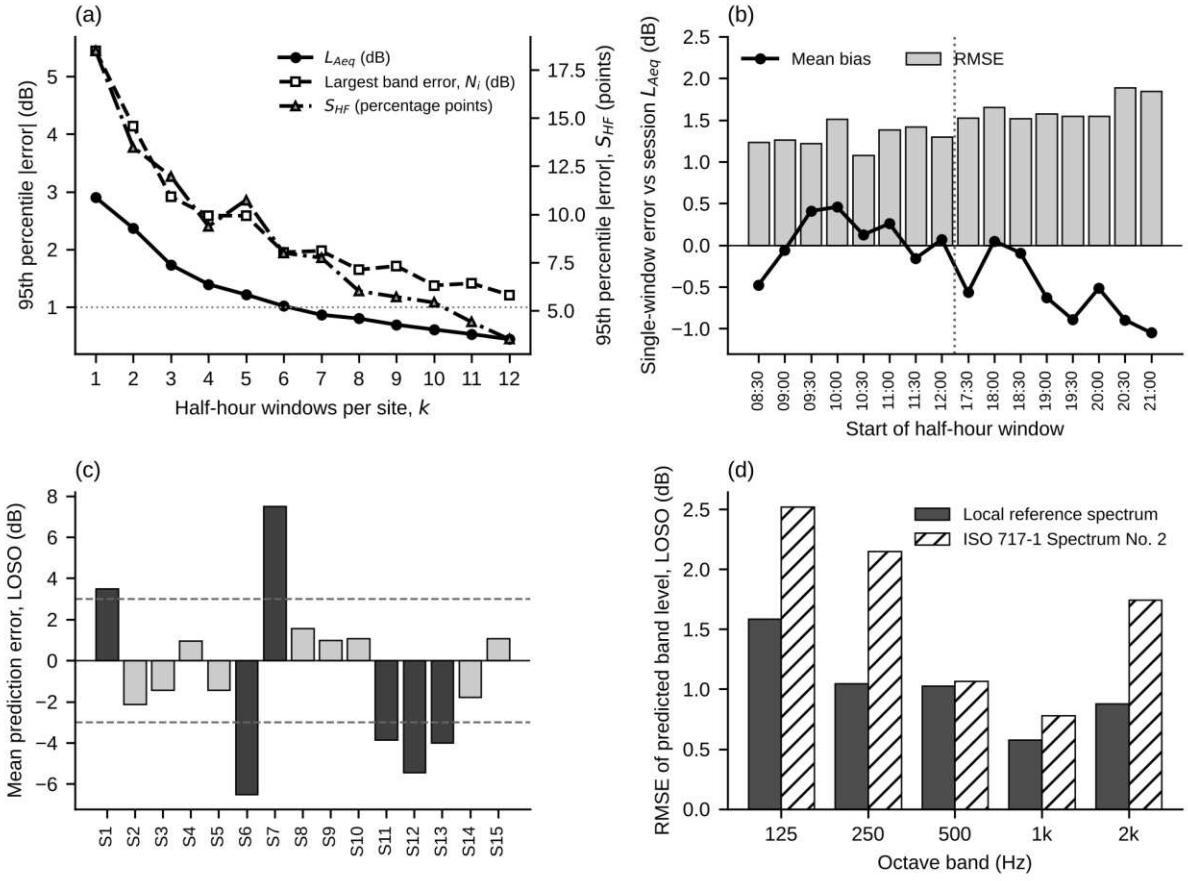

Fig. 12 Monitoring design: (a) 95th-percentile sampling error against the number of half-hour windows; (b) bias and RMSE of single half-hour windows as estimates of the session level; (c) mean leave-one-site-out error of the flow-and-composition model at each site (dark bars exceed ±3 dB); (d) leave-one-site-out RMSE of band levels predicted from L_{Aeq} with the local reference spectrum and with ISO 717-1 Spectrum No. 2

3.9 Consequence for spectrum-adapted ratings

For the three generic elements, X_A computed with the measured spectrum over 125 Hz–2 kHz exceeded the value obtained with ISO 717-1 Spectrum No. 2 by 1.6 dB for the mass-law element, 0.1 dB for glazing with a 2 kHz coincidence dip and 2.0 dB for the double-leaf element. Including the 4 kHz band raised these margins to 3.3, 1.5 and 3.7 dB (Fig. 13). For elements whose insulation increases with frequency, C_{tr} therefore understates the protection achieved against this noise. The margin narrows sharply for elements with a coincidence dip in the 2–4 kHz region, precisely where heterogeneous traffic concentrates its energy.

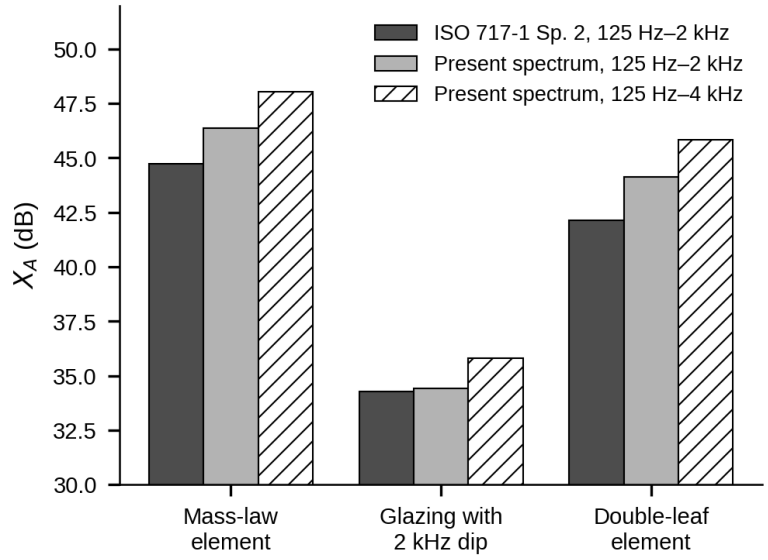

Fig. 13 A-weighted level reduction X_A of three generic building elements computed with ISO 717-1 Spectrum No. 2 and with the measured spectrum over 125 Hz–2 kHz and 125 Hz–4 kHz

4 Discussion

4.1 Comparison with earlier studies

Table 12 sets the present findings against reference spectra and earlier work. The scale of non-compliance agrees with national network data, which have shown most monitoring stations in seven major cities above their limits (N. Garg et al. 2017; Naveen Garg et al. 2017) ; the present analysis adds that, at intersections, the exceedance survives a full allowance for measurement uncertainty at 13 of 15 sites. European reference spectra peak near 1 kHz (European Committee for Standardization 1997; Sandberg and Ejsmont 2002) , whereas the Surat spectrum peaks at 4 kHz at four out of five sites. Indian studies that examined spectra point the same way: Vijay et al. (Vijay et al. 2015) located honking energy in the 2 and 4 kHz octaves in Nagpur, and horn-related increments of several decibels recur across the literature (Kalaiselvi and

Ramachandraiah 2016; Sonaviya and Tandel 2020; Thakre et al. 2020) . The weak response of level to flow within sites agrees with the poor volume–level correlations reported for Surat (R. Sonaviya and N. Tandel 2021; Sonaviya and Tandel 2020) , and the present design shows that this weakness is confined to temporal variation at a site: across sites, level still follows flow as theory predicts. It also explains why locally calibrated models in Indian cities have had to rely on site-specific terms or flexible learners (Chouksey et al. 2023; Yadav et al. 2024) , and why their transfer to new sites remains an open question.

Table 12 Comparison of the present findings with reference spectra and published studies

Source	Setting	Reported finding	Present study
EN 1793-3 (European Committee for Standardization 1997)	European roads, normalised spectrum	Maximum weight in the 1 kHz band	Maximum in the 4 kHz band at 12 of 15 sites
ISO 717-1 Sp. 2 (International Organization for Standardization 2020)	Urban road traffic (C_{tr})	Octave rating range 125 Hz–2 kHz	Median 41% of A-weighted energy at 4–8 kHz
Sandberg and Ejsmont (Sandberg and Ejsmont 2002)	Free-flowing traffic, tyre–road noise	Broad maximum near 1 kHz, decline above	Unweighted local maximum at 4 kHz
Garg et al. (Naveen Garg et al. 2017)	National network, seven cities	Most stations above limits; few industrial sites compliant	13 of 15 sites exceed beyond *U*; industrial S6 complies
Vijay et al. (Vijay et al. 2015)	Nagpur, three road types	Honking energy in 500 Hz, 2 and 4 kHz octaves; +2–5 dB(A)	Consistent with 2–4 kHz excess
Kalaiselvi and Ramachandraiah (Kalaiselvi and Ramachandraiah 2016)	Indian heterogeneous traffic	Horn events add 0.5–13 dB(A)	High-frequency share independent of flow
Sonaviya and Tandel (Sonaviya and Tandel 2020)	Surat road network	Weak correlation of L_{eq} with volume	Within-site slope 0.18 against 1.0 expected
Prieto Gajardo and Barrigón Morillas (Prieto Gajardo and Barrigón Morillas 2015)	Urban sites, Spain	Stabilisation of hourly levels governs short-term sampling	±1 dB requires seven half-hour windows

4.2 Why level does not follow flow at an intersection

Two mechanisms explain the weak within-site slope. First, a signalised intersection operates close to capacity for much of the day. Additional vehicles lengthen queues and discharge periods rather than adding independent pass-bys, so the sound energy per vehicle falls as flow rises; acceleration and deceleration, not the vehicle count alone, govern emission at such locations (Can and Aumond 2018) . The between-site behaviour of L_{min} and L_{max} supports this reading: heavier flow raises the floor of the noise but not its peaks, which is the acoustic signature of continuous idling and stop-and-go movement. Secondly, a substantial part of the energy comes from a source that does not scale with vehicle numbers. The late-evening slots illustrate this plainly: as flow fell to its daily minimum, level barely changed and the high-frequency share reached its maximum.

4.3 Origin of the high-frequency component

The high-frequency component behaves in a distinctive way. It is independent of flow and of every vehicle share, yet it differs persistently between intersections, dominates the principal axis of spectral variation and defines the spectral site types. Rolling and propulsion noise scale with the number and type of vehicles, so neither can account for it. Horn use fits all of these features: it depends on driver behaviour, signal operation, parking and conflicts at the junction rather than on flow (Kalaiselvi and Ramachandraiah 2016; Sonaviya and Tandel 2020) , and its energy falls in the 2–4 kHz octaves (Vijay et al. 2015) . The low share at the educational site, where horn use is restricted near educational institutions (Ministry of Environment and Forests 2000) , is consistent with this interpretation, although a single site cannot establish it. Brake squeal and two-wheeler engine noise may add to the component (Paviotti and Vogiatzis 2012) . Synchronised horn counts or short-interval recordings would allow the contribution of each source to be separated.

Instrument response must also be considered. The same class 2 meter was used at every site, and the acceptance limits of IEC 61672-1 for class 2 instruments widen at 4 and 8 kHz relative to the mid-frequency range (International Electrotechnical Commission 2002) . A systematic response deviation at 4 kHz would shift all spectra by the same amount and could contribute to the absolute 4 kHz level. It cannot, however, generate the differences in high-frequency share between sites, the principal component and cluster structure or the absence of any relation with traffic, since a constant offset leaves all of these unchanged.

4.4 Implications for monitoring and assessment

The results translate into five recommendations for monitoring at intersections carrying heterogeneous traffic. First, compliance should be reported with its uncertainty. At most sites the margin is so large that the conclusion is robust, but at sites close to their limit, such as S7, a single number without uncertainty would overstate the certainty of non-compliance. Secondly, short surveys should comprise at least seven half-hour windows spread over the morning and evening peaks for a ±1 dB estimate, three windows for ±2 dB and about eleven windows when spectral balance is to be characterised; a single late-evening window should not be used, because it understates peak-period levels by about 1 dB. Thirdly, flow-based prediction should not replace measurement at individual intersections. The site-level biases of up to 7.5 dB exceed the margin by which most sites exceed their limits and would misclassify compliance; models calibrated elsewhere, whether in another city or another country, carry the

same risk (Peng et al. 2018) . Fourthly, when only broadband levels are available, band levels for façade design, barrier assessment or noise mapping (N. Garg et al. 2021; Sonaviya and Tandel 2019) can be estimated from L_{Aeq} with the local reference spectrum to within about 1–1.6 dB below 2 kHz, appreciably better than with the ISO spectrum. Finally, since spectral type is a stable property of a site and is not predicted by traffic or land use, a short octave-band survey at each intersection is the most direct way to identify locations where high-frequency, behaviour-related noise dominates and where horn restrictions, signal coordination and enforcement against obstructive parking are likely to yield more than measures aimed at flow.

For façade design near intersections, ratings based on C_{tr} are conservative for typical constructions, but glazing and lightweight panels with coincidence dips at 2–4 kHz should be assessed against the measured spectrum. The reference spectrum in Table 5 and the type spectra in Table 8 can be used directly in spectrum-adapted assessments for Indian cities.

4.5 Limitations

Octave rather than one-third-octave bands were measured, which precludes a band-by-band comparison with the one-third-octave forms of ISO 717-1 and EN 1793-3. Measurements were made at the kerb rather than at façades, and the session covered the two daily peaks rather than the full statutory daytime period, so session levels indicate peak-period exposure. The instrumental uncertainty was assigned from standard guidance rather than determined for the specific instrument. The sampling errors are relative to a single-day session and do not include day-to-day variation, which would add to them. The peri-urban sites contributed four windows each, and several land-use categories were represented by a single site, so land-use differences remain descriptive.

5 Conclusions

Octave-band monitoring at 15 signalised intersections in Surat establishes that heterogeneous intersection traffic produces noise that exceeds national daytime limits beyond measurement uncertainty at 13 of 15 sites, with a stable A-weighted spectrum whose maximum lies at 4 kHz. The principal findings are as follows.

(i) Relative to ISO 717-1 Spectrum No. 2, the measured spectrum carries 1.8–2.3 dB less energy at 125–250 Hz and 1.7 dB more at 2 kHz, and a median 41% of its A-weighted energy lies in the 4 and 8 kHz bands, outside the octave rating range.

(ii) The balance between high and low frequencies is the dominant mode of spectral variation, is a stable property of each intersection, is independent of traffic flow and composition, and divides the sites into three spectral types that do not follow land use.

(iii) Flow varied 3.4-fold over the day while median level varied by 2.8 dB; within an intersection, level rises by only about 0.5 dB per doubling of flow in every octave band, while between intersections higher flow lifts the noise floor twice as steeply as theory predicts and compresses the dynamic range.

(iv) A flow-and-composition model transferred to unseen sites with an error of 3.8 dB and site biases up to 7.5 dB, whereas the local reference spectrum predicted band levels from L_{Aeq} within 0.6–1.6 dB over 125 Hz–2 kHz and outperformed the ISO spectrum in every band.

(v) Seven half-hour windows are needed to estimate a peak-period level within ±1 dB, and late-evening windows understate it by about 1 dB.

Intersection noise in Indian cities is therefore governed as much by behaviour and junction operation as by traffic volume. Its assessment should rest on site measurement of adequate duration, reported with uncertainty, and spectrum-adapted evaluations should adopt locally derived spectra such as those reported here.

Statements and declarations

Funding The authors declare that no funds, grants or other support were received during the preparation of this manuscript.

Competing interests The authors have no relevant financial or non-financial interests to disclose.

Author contributions Conceptualization: Bhaven N. Tandel, Manoranjan Parida; Data curation: Bhanu Chaudhary; Formal analysis: Bhanu Chaudhary; Investigation: Bhanu Chaudhary; Methodology: Bhanu Chaudhary, Bhaven N. Tandel; Project administration: Bhaven N. Tandel; Resources: Bhaven N. Tandel; Software: Bhanu Chaudhary; Supervision: Bhaven N. Tandel, Manoranjan Parida; Validation: Bhaven N. Tandel, Manoranjan Parida; Visualization: Bhanu Chaudhary; Writing – original draft: Bhanu Chaudhary; Writing – review and editing: Bhanu Chaudhary, Bhaven N. Tandel, Manoranjan Parida. All authors read and approved the final manuscript.

Data availability The data supporting the findings of this study are available from the corresponding author on reasonable request.

Ethics approval Not applicable. The study involved environmental measurements only; video recordings were used solely for vehicle counting and no individuals were identified.

Consent to participate and for publication Not applicable.

Use of generative AI During the preparation of this work the authors used Claude (Anthropic) to assist with language editing of the manuscript. The authors reviewed, edited and take full responsibility for the content of the publication.

Acknowledgements The authors thank the Surat Traffic Police Department for permission to conduct field measurements at the selected intersections.

Appendix A Supplementary analyses

Table A1 repeats the principal models with the three peri-urban sites excluded. The within-site slope of L_{Aeq} and the median high-frequency share are unchanged, whereas the between-site slope falls to 0.51 and loses significance, showing that the between-site relation rests largely on the contrast between urban and peri-urban sites. Table A2 gives pooled Spearman rank correlations between the main variables.

Table A1 Sensitivity of the main results to the exclusion of peri-urban sites

Sample	Within-site slope, L_{Aeq} (p)	Between-site slope, L_{Aeq} (p)	Within-site slope, S_{HF} (p)	Median S_{HF} (%)
All sites (S1–S15)	0.18 (0.009)	0.95 (<0.001)	0.10 (0.789)	40.8
Urban sites only (S1–S10, S14, S15)	0.18 (0.010)	0.51 (0.101)	0.17 (0.673)	41.0

Table A2 Spearman rank correlations between acoustic and traffic variables (203 windows)

	L_{Aeq}	L_{max}	L_{min}	NC	PCU	2W	3W	4W	HV	S_{HF}	f_c
L_{Aeq}	1										
L_{max}	0.72	1									
L_{min}	0.66	0.41	1								
NC	0.01	0.46	−0.53	1							
PCU	0.42	0.24	0.46	−0.22	1						
2W	0.01	−0.04	−0.01	0.01	−0.08	1					
3W	0.07	0.13	−0.01	0.10	−0.23	−0.37	1				
4W	−0.05	−0.13	0.03	−0.17	0.16	−0.10	−0.72	1			
HV	0.12	0.20	0.12	0.11	0.27	−0.36	−0.25	0.21	1		
S_{HF}	0.60	0.42	0.36	0.06	0.08	−0.01	0.07	0.04	0.00	1	

	L_{Aeq}	L_{max}	L_{min}	NC	PCU	2W	3W	4W	HV	S_{HF}	f_c
f_c	0.54	0.41	0.32	0.11	0.06	0.00	0.06	0.03	−0.01	0.98	1

NC = $L_{max} - L_{min}$; 2W, 3W, 4W and HV are percentage shares; f_c spectral centroid

References

Banerjee, D., Chakraborty, S. K., Bhattacharyya, S., & Gangopadhyay, A. (2008). Evaluation and Analysis of Road Traffic Noise in Asansol: An Industrial Town of Eastern India. *International Journal of Environmental Research and Public Health*, *5*(3), 165–171. https://doi.org/10.3390/ijerph5030165

Basner, M., Babisch, W., Davis, A., Brink, M., Clark, C., Janssen, S., & Stansfeld, S. (2014). Auditory and non-auditory effects of noise on health. *The Lancet*, *383*(9925), 1325–1332. https://doi.org/10.1016/S0140-6736(13)61613-X

Bell, A., & Jones, K. (2015). Explaining Fixed Effects: Random Effects Modeling of Time-Series Cross-Sectional and Panel Data. *Political Science Research and Methods*, *3*(1), 133–153. https://doi.org/10.1017/psrm.2014.7

Benjamini, Y., & Hochberg, Y. (1995). Controlling the False Discovery Rate: A Practical and Powerful Approach to Multiple Testing. *Journal of the Royal Statistical Society Series B: Statistical Methodology*, *57*(1), 289–300. https://doi.org/10.1111/j.2517-6161.1995.tb02031.x

Berglund, B., Hassmén, P., & Job, R. F. S. (1996). Sources and effects of low-frequency noise. *The Journal of the Acoustical Society of America*, *99*(5), 2985–3002. https://doi.org/10.1121/1.414863

Can, A., & Aumond, P. (2018). Estimation of road traffic noise emissions: The influence of speed and acceleration. *Transportation Research Part D: Transport and Environment*, *58*, 155–171. https://doi.org/10.1016/j.trd.2017.12.002

Can, A., Leclercq, L., Lelong, J., & Botteldooren, D. (2010). Traffic noise spectrum analysis: Dynamic modeling vs. experimental observations. *Applied Acoustics*, *71*(8), 764–770. https://doi.org/10.1016/j.apacoust.2010.04.002

Chouksey, A. K., Kumar, B., Parida, M., Pandey, A. D., & Verma, G. (2023). Heterogeneous road traffic noise modeling at mid-block sections of mid-sized city in India. *Environmental Monitoring and Assessment*, *195*(11), 1349. https://doi.org/10.1007/s10661-023-11924-0

Dhamaniya, A., & Chandra, S. (2013). Concept of Stream Equivalency Factor for Heterogeneous Traffic on Urban Arterial Roads. *Journal of Transportation Engineering*, *139*(11), 1117–1123. https://doi.org/10.1061/(ASCE)TE.1943-5436.0000581

Efron, B., & Tibshirani, R. J. (1993). *An Introduction to the Bootstrap*. Boston, MA: Springer US. https://doi.org/10.1007/978-1-4899-4541-9

ephalopoulos, S., Paviotti, M., & Anfosso-Lédée, F. (2012). *Common Noise Assessment Methods in Europe (CNOSSOS-EU)*.

European Committee for Standardization. (1997). *EN 1793-3:1997 Road traffic noise reducing devices — Test method for determining the acoustic performance — Part 3: Normalized traffic noise spectrum*. Brussels.

Gaja, E., Gimenez, A., Sancho, S., & Reig, A. (2003). Sampling techniques for the estimation of the annual equivalent noise level under urban traffic conditions. *Applied Acoustics*, *64*(1), 43–53. https://doi.org/10.1016/S0003-682X(02)00050-6

Garg, N., Chauhan, B. S., & Singh, M. (2021). Normative Framework of Noise Mapping in India: Strategies, Implications and Challenges Ahead. *Acoustics Australia*, *49*(1), 23–41. https://doi.org/10.1007/s40857-020-00214-1

Garg, N., Sinha, A. K., Gandhi, V., Bhardwaj, R. M., & Akolkar, A. B. (2016). A pilot study on the establishment of national ambient noise monitoring network across the major cities of India. *Applied Acoustics*, *103*, 20–29. https://doi.org/10.1016/j.apacoust.2015.09.010

Garg, N., Sinha, A. K., Sharma, M. K., Gandhi, V., Bhardwaj, R. M., Akolkar, A. B., & Singh, R. K. (2017). Study on the Establishment of a Diversified National Ambient Noise Monitoring Network in Seven Major Cities of India. *Current Science*, *113*(07), 1367. https://doi.org/10.18520/cs/v113/i07/1367-1383

Garg, Naveen, & Maji, S. (2014). A critical review of principal traffic noise models: Strategies and implications. *Environmental Impact Assessment Review*, *46*, 68–81. https://doi.org/10.1016/j.eiar.2014.02.001

Garg, Naveen, Sinha, A. K., Dahiya, M., Gandhi, V., Bhardwaj, R. M., & Akolkar, A. B. (2017). Evaluation and Analysis of Environmental Noise Pollution in Seven Major Cities of India. *Archives of Acoustics*, *42*(2), 175–188. https://doi.org/10.1515/aoa-2017-0020

Heutschi, K. (2004). SonRoad: New Swiss road traffic noise model. *Acta Acustica united with Acustica*, *90*(3), 548–554.

Hollander, M., A. Wolfe, D., & Chicken, E. (2015). *Nonparametric Statistical Methods*. Wiley. https://doi.org/10.1002/9781119196037

International Electrotechnical Commission. (2002). *IEC 61672-1:2002 Electroacoustics — Sound level meters — Part 1: Specifications*. Geneva.

International Electrotechnical Commission. (2014). *IEC 61260-1:2014 Electroacoustics — Octave-band and fractional-octave-band filters — Part 1: Specifications*. Geneva.

International Organization for Standardization. (2017). *ISO 1996-2:2017 Acoustics — Description, measurement and assessment of environmental noise — Part 2: Determination of sound pressure levels* . Geneva.

International Organization for Standardization. (2020). *ISO 717-1:2020 Acoustics — Rating of sound insulation in buildings and of building elements — Part 1: Airborne sound insulation*. Geneva.

Joint Committee for Guides in Metrology. (2012). *JCGM 106:2012 Evaluation of measurement data — The role of measurement uncertainty in conformity assessment*.

Jolliffe, I. T., & Cadima, J. (2016). Principal component analysis: a review and recent developments. *Philosophical Transactions of the Royal Society A: Mathematical, Physical and Engineering Sciences*, *374*(2065), 20150202. https://doi.org/10.1098/rsta.2015.0202

Jonasson, H. G. (2007). Acoustical source modelling of road vehicles. *Acta Acustica united with Acustica*, *93*(2), 173–184.

Kalaiselvi, R., & Ramachandraiah, A. (2016). Honking noise corrections for traffic noise prediction models in heterogeneous traffic conditions like India. *Applied Acoustics*, *111*, 25–38. https://doi.org/10.1016/j.apacoust.2016.04.003

Koo, T. K., & Li, M. Y. (2016). A Guideline of Selecting and Reporting Intraclass Correlation Coefficients for Reliability Research. *Journal of Chiropractic Medicine*, *15*(2), 155–163. https://doi.org/10.1016/j.jcm.2016.02.012

Ministry of Environment and Forests, G. of I. The Noise Pollution (Regulation and Control) Rules, 2000. , Pub. L. No. S.O. 123(E) (2000). Gazette of India, Extraordinary.

Mishra, R. K., Parida, M., & Rangnekar, S. (2010). Evaluation and analysis of traffic noise along bus rapid transit system corridor. *International Journal of Environmental Science & Technology*, *7*(4), 737–750. https://doi.org/10.1007/BF03326183

oint Committee for Guides in Metrology. (2008). *JCGM 100:2008 Evaluation of measurement data — Guide to the expression of uncertainty in measurement*.

Pathak, V., Tripathi, B. D., & Mishra, V. kumar. (2008). Evaluation of traffic noise pollution and attitudes of exposed individuals in working place. *Atmospheric Environment*, *42*(16), 3892–3898. https://doi.org/10.1016/j.atmosenv.2007.12.070

Paviotti, M., & Vogiatzis, K. (2012). On the outdoor annoyance from scooter and motorbike noise in the urban environment. *Science of The Total Environment*, *430*, 223–230. https://doi.org/10.1016/j.scitotenv.2012.05.010

Peng, J., Parnell, J., & Kessissoglou, N. (2018). Adoption of an offshore developed road traffic noise prediction model. In *Proceedings of the 13th Western Pacific Acoustics Conference (WESPAC 2018), New Delhi, India*.

Prieto Gajardo, C., & Barrigón Morillas, J. M. (2015). Stabilisation patterns of hourly urban sound levels. *Environmental Monitoring and Assessment*, *187*(1), 4072. https://doi.org/10.1007/s10661-014-4072-3

R. Sonaviya, D., & N. Tandel, B. (2021). Prediction and Limitations of Noise Maps Developed for Heterogeneous Urban Road Traffic Condition: A Case Study of Surat City, India. *Sound&Vibration*, *55*(1), 57–68. https://doi.org/10.32604/sv.2021.010715

Rajakumara, H. N., & Mahalinge Gowda, R. M. (2009). Road Traffic Noise Prediction Model under Interrupted Traffic Flow Condition. *Environmental Modeling & Assessment*, *14*(2), 251–257. https://doi.org/10.1007/s10666-008-9138-6

699 Rousseeuw, P. J. (1987). Silhouettes: A graphical aid to the interpretation and validation of cluster
700 analysis. *Journal of Computational and Applied Mathematics*, *20*, 53–65.
701 https://doi.org/10.1016/0377-0427(87)90125-7
702 Sandberg, U., & Ejsmont, J. A. (2002). *Tyre/Road Noise Reference Book*. Sweden: Informex, Kisa.
703 Scholl, W., Lang, J., & Wittstock, V. (2011). Rating of sound insulation at present and in future. The
704 revision of ISO 717. *Acta Acustica united with Acustica*, *97*(4), 686–698.
705 Seabold, S., & Perktold, J. (2010). Statsmodels: Econometric and Statistical Modeling with Python (pp.
706 92–96). https://doi.org/10.25080/Majora-92bf1922-011
707 Sonaviya, D. R., & Tandel, B. N. (2019). A Review on GIS-Based Approach for Road Traffic Noise
708 Mapping. *Indian Journal of Science and Technology*, *14*(12), 1–6.
709 https://doi.org/10.17485/ijst/2019/v12i14/132481
710 Sonaviya, D. R., & Tandel, B. N. (2020). Integrated road traffic noise mapping in urban Indian context.
711 *Noise Mapping*, *7*(1), 99–113. https://doi.org/10.1515/noise-2020-0009
712 Thakre, C., Laxmi, V., Vijay, R., Killedar, D. J., & Kumar, R. (2020). Traffic noise prediction model
713 of an Indian road: an increased scenario of vehicles and honking. *Environmental Science and*
714 *Pollution Research*, *27*(30), 38311–38320. https://doi.org/10.1007/s11356-020-09923-6
715 Torija, A. J., & Flindell, I. H. (2014). Differences in subjective loudness and annoyance depending on
716 the road traffic noise spectrum. *The Journal of the Acoustical Society of America*, *135*(1), 1–4.
717 https://doi.org/10.1121/1.4842456
718 Torija, A. J., Ruiz, D. P., & Ramos-Ridao, Á. (2011). Required stabilization time, short-term variability
719 and impulsiveness of the sound pressure level to characterize the temporal composition of urban
720 soundscapes. *Applied Acoustics*, *72*(2–3), 89–99. https://doi.org/10.1016/j.apacoust.2010.09.011
721 Vijay, R., Sharma, A., Chakrabarti, T., & Gupta, R. (2015). Assessment of honking impact on traffic
722 noise in urban traffic environment of Nagpur, India. *Journal of Environmental Health Science and*
723 *Engineering*, *13*(1), 10. https://doi.org/10.1186/s40201-015-0164-4
724 Ward, J. H. (1963). Hierarchical Grouping to Optimize an Objective Function. *Journal of the American*
725 *Statistical Association*, *58*(301), 236–244. https://doi.org/10.1080/01621459.1963.10500845
726 World Health Organization Regional Office for Europe. (2018). *Environmental Noise Guidelines for*
727 *the European Region*.
728 Yadav, A., Parida, M., Choudhary, P., Kumar, B., & Singh, D. (2024). Traffic noise modelling at
729 intersections in mid-sized cities: an artificial neural network approach. *Environmental Monitoring*
730 *and Assessment*, *196*(4), 396. https://doi.org/10.1007/s10661-024-12547-9
731